



**HAL**  
open science

# Molecular characterization of dopamine-derived quinones reactivity toward NADH and glutathione: Implications for mitochondrial dysfunction in Parkinson disease

Marco Bisaglia, Maria Eugenia Soriano, Irene Arduini, Stefano Mammi, Luigi Bubacco

## ► To cite this version:

Marco Bisaglia, Maria Eugenia Soriano, Irene Arduini, Stefano Mammi, Luigi Bubacco. Molecular characterization of dopamine-derived quinones reactivity toward NADH and glutathione: Implications for mitochondrial dysfunction in Parkinson disease. *Biochimica et Biophysica Acta - Molecular Basis of Disease*, 2010, 1802 (9), pp.699. 10.1016/j.bbadis.2010.06.006 . hal-00608985

**HAL Id: hal-00608985**

**<https://hal.science/hal-00608985>**

Submitted on 17 Jul 2011

**HAL** is a multi-disciplinary open access archive for the deposit and dissemination of scientific research documents, whether they are published or not. The documents may come from teaching and research institutions in France or abroad, or from public or private research centers.

L'archive ouverte pluridisciplinaire **HAL**, est destinée au dépôt et à la diffusion de documents scientifiques de niveau recherche, publiés ou non, émanant des établissements d'enseignement et de recherche français ou étrangers, des laboratoires publics ou privés.

## Accepted Manuscript

Molecular characterization of dopamine-derived quinones reactivity toward NADH and glutathione: Implications for mitochondrial dysfunction in Parkinson disease

Marco Bisaglia, Maria Eugenia Soriano, Irene Arduini, Stefano Mammi, Luigi Bubacco

PII: S0925-4439(10)00116-X  
DOI: doi: [10.1016/j.bbadis.2010.06.006](https://doi.org/10.1016/j.bbadis.2010.06.006)  
Reference: BBADIS 63114

To appear in: *BBA - Molecular Basis of Disease*

Received date: 20 October 2009  
Revised date: 4 June 2010  
Accepted date: 10 June 2010



Please cite this article as: Marco Bisaglia, Maria Eugenia Soriano, Irene Arduini, Stefano Mammi, Luigi Bubacco, Molecular characterization of dopamine-derived quinones reactivity toward NADH and glutathione: Implications for mitochondrial dysfunction in Parkinson disease, *BBA - Molecular Basis of Disease* (2010), doi: [10.1016/j.bbadis.2010.06.006](https://doi.org/10.1016/j.bbadis.2010.06.006)

This is a PDF file of an unedited manuscript that has been accepted for publication. As a service to our customers we are providing this early version of the manuscript. The manuscript will undergo copyediting, typesetting, and review of the resulting proof before it is published in its final form. Please note that during the production process errors may be discovered which could affect the content, and all legal disclaimers that apply to the journal pertain.

**Molecular characterization of dopamine-derived quinones reactivity toward NADH and glutathione: implications for mitochondrial dysfunction in Parkinson disease.**

Marco Bisaglia<sup>a, 1</sup>, Maria Eugenia Soriano<sup>b, 1</sup>, Irene Arduini<sup>a</sup>, Stefano Mammi<sup>c</sup>, and Luigi Bubacco<sup>a\*</sup>

<sup>a</sup> Department of Biology, University of Padova, Padova, Italy

<sup>b</sup> Department of Biomedical Sciences/C.N.R. Institute of Neurosciences, University of Padova

<sup>c</sup> Department of Chemical Sciences/C.N.R. Institute of Biomolecular Chemistry, University of Padova, Padova, Italy

<sup>1</sup> These authors contributed equally to the work.

\* Corresponding author: Luigi Bubacco, Department of Biology, University of Padova, Via Ugo Bassi 58B, 35121 Padova, Italy. Tel: +390498276346; Fax: +390498276300; E-mail: [luigi.bubacco@unipd.it](mailto:luigi.bubacco@unipd.it)

Keywords: Dopamine quinones, glutathione, mitochondria, NADH, NMR

**ABSTRACT**

Oxidative stress and mitochondrial dysfunction, especially at the level of complex I of the electronic transport chain, have been proposed to be involved in the pathogenesis of Parkinson disease (PD). A plausible source of oxidative stress in nigral dopaminergic neurons is the redox reactions that specifically involve dopamine (DA) and produce various toxic molecules, i.e., free radicals and quinone species (DAQ). It has been shown that DA oxidation products can induce various forms of mitochondrial dysfunction, such as mitochondrial swelling and decreased electron transport chain activity.

In the present work, we analyzed the potentially toxic effects of DAQ on mitochondria and, specifically, on the NADH and GSH pools. Our results demonstrate that the generation of DAQ in isolated respiring mitochondria triggers the opening of the permeability transition pore most probably by inducing oxidation of NADH, while GSH levels are not affected. We then characterized *in vitro*, by UV and NMR spectroscopy, the reactivity of different DA-derived quinones, i.e., dopamine-o-quinone (DQ), aminochrome (AC) and indole-quinone (IQ), toward NADH and GSH. Our results indicate a very diverse reactivity for the different DAQ studied that may contribute to unravel the complex molecular mechanisms underlying oxidative stress and mitochondria dysfunction in the context of PD.

Parkinson disease (PD) is the second most common central nervous system disorder. The estimated prevalence in 2005 was more than four million people in the world's most populous countries and it is expected to more than double by 2030, as worldwide life expectancy continues to rise [1].

Various groups of neurons exhibit pathology in PD, and extensive (~80%) neuronal death has been reported for substantia nigra (SN) dopaminergic and locus coeruleus norepinephrinergic neurons. Nevertheless, while locus coeruleus neuron death is elevated also in Alzheimer disease, the most common neurodegenerative disorder, the loss of SN dopaminergic neurons seems specific to PD [2].

Although the etiopathogenesis of PD is still elusive, *post mortem* studies support the involvement of oxidative stress in neuronal damage, through the production of reactive oxygen species, and of mitochondrial dysfunction, especially at the level of complex I of the electron transport chain [3-6]. The coexistence of mitochondrial dysfunction and oxidative stress with nigral cell loss in PD brains and experimental models makes it difficult to establish whether the former are causes or consequences of nigral degeneration. What is clear, on the contrary, is that oxidative stress and mitochondrial dysfunction appear to be strictly correlated and to influence each other.

In the aforementioned vulnerability of dopaminergic neurons in PD, DA itself could represent a crucial determinant. The redox reactions that specifically involve cytosolic DA and generate the superoxide anion, hydrogen peroxide and quinones (DAQ) [7] are indeed a possible source of oxidative stress. It has been shown that DA oxidation products, including DAQ, can induce various forms of mitochondrial dysfunction, such as swelling and decreased electron transport chain activity [8-11].

Dopaminergic neurons have evolved multiple protective mechanisms against cytosolic DA toxicity. These include feedback synthesis inhibition, synaptic vesicle or lysosome sequestration, degradation by monoamine oxidase and reduction of DAQ by glutathione (GSH). The latter is the most abundant intracellular non protein thiol compound in mammalian cells, reaching concentrations up to 12 mM [12]. Interestingly, it has been observed that there is an age-dependent depletion in intracellular GSH [13] and that SN has lower levels of GSH compared to other brain regions, according to the following order: cortex > cerebellum > hippocampus > striatum > SN [14]. Additionally, a further specific decrease in GSH levels has been reported in the SN of early and advanced PD patients, compared with aged controls, suggesting the decrease of GSH levels in the SN as an early event for PD [15-17]. Therefore, changes in GSH levels may crucially affect the ability of SN cells to cope with free radical species or DAQ. At the same time, the defense mechanisms could be overwhelmed by the redistribution to the cytosol of the DA from the synaptic

vesicles where it is stored at a concentration approximately five orders of magnitude higher [2]. A major source of reactive oxygen species (ROS) in the cell are the mitochondria, which also contain several antioxidant tools, such as superoxide dismutase (SOD2), and protective molecules such as GSH. The redox state of glutathione is in part regulated by the redox state of the pyridine nucleotide (PN) pool and the activity of glutathione reductase and peroxidase enzymes. The unbalance in the redox equilibrium inside mitochondria can lead to mitochondrial dysfunction and, specifically, the oxidized forms of pyridine nucleotides and glutathione favor the permeability transition (PT) [18, 19]. The PT in turn causes mitochondrial depolarization swelling and release of proapoptotic proteins that activate cell death.

In the present work, we focused on the potentially toxic effects of DAQ on mitochondria and, specifically, on the NADH and GSH pools. Our results demonstrate that the generation of DAQ in isolated respiring mitochondria triggers the opening of the permeability transition pore most probably by inducing oxidation of NADH. We then characterized *in vitro*, by UV and NMR spectroscopy, the reactivity of different DA-derived quinones, i.e., dopamine-o-quinone (DQ), aminochrome (AC) and indole-quinone (IQ), toward NADH. We also took into account the protective role exerted by GSH. The results presented here indicate a very diverse behaviour for the different DAQ studied and may contribute to unravel the complex molecular mechanisms underlying oxidative stress and mitochondrial dysfunction in the context of PD. Specifically, DQ and IQ are very reactive with both NADH and GSH and the reaction with GSH is largely favoured. On the contrary, AC does not show any apparent reactivity.

AC

## Materials and Methods

*Chemicals* – Cyclosporin A (CsA), dopamine, reduced L-glutathione, nicotinamide adenine dinucleotide, sodium phosphate salt and mushroom tyrosinase (Ty) were purchased from Sigma-Aldrich. Water-d<sub>2</sub> and sodium 3-trimethylsilyl propionate-2,2,3,3-d<sub>4</sub> (TSP) were obtained from Cambridge Isotope Laboratories.

*Mouse liver mitochondria isolation* - Mitochondria were isolated from CD1 mice by a standard procedure as described in Costantini et al. [20] with some modifications. Briefly, the liver was minced in a buffer containing 0.25 M sucrose, 10 mM Tris-HCl (pH 7.4) and 0.1 mM EGTA. The minced liver was homogenized in the same buffer and centrifuged at 700 x g for 6 min. The supernatant was centrifuged at 7000 x g for 6 min. The resulting mitochondrial pellet was resuspended and recentrifuged at 7000 x g for 6 min. The entire procedure was carried out at 4 °C. Mitochondrial protein concentration was determined by the biuret reaction with BSA as a standard.

*Mitochondrial swelling* - Mitochondrial swelling was followed as the change of light scattering of the mitochondrial suspension at 620 nm with a Perkin-Elmer Life Sciences 650-40 fluorescence spectrophotometer equipped with magnetic stirring and thermostatic control. Mitochondria (1 mg, 0.5 mg/ml) were incubated in 2 ml of medium containing 0.25 M sucrose, 10 mM Tris-MOPS, 1 mM Pi-Tris, 10 μM EGTA-Tris, 5 mM glutamate/2.5 mM malate or 5 mM succinate-Tris plus 2 μM rotenone. An amount of Ca<sup>2+</sup> under the threshold necessary to trigger PT was added to accelerate PT by subsequent treatments. Alkylating reagents such as monobromobimane (MBB) or N-ethylmaleimide (NEM) were added after 1 minute. DA (100 μM) and Ty (120 units) were added to the solution after another minute. When CsA (0.8 μM) was used, it was added in the medium before the addition of mitochondria.

*Pyridine Nucleotide Assay* - Mitochondria (1.5 mg, 0.5 mg/ml) were incubated for 10 min at room temperature (RT) in the presence of 60 μM DA and 100 units of Ty to generate DAQ in a medium containing 0.25 M sucrose, 10 mM Tris-MOPS, 5 mM succinate, 1 mM inorganic phosphate, 10 μM EGTA, 2 μM rotenone and 0.8 μM CsA to avoid pyridine nucleotides release from mitochondria due to PT during the reaction between DA and Ty. To eliminate the coloured quinones, mitochondria were centrifuged at 6000 x g and 4 °C for 6 min and then gently resuspended in 3 ml of the same medium. NADH was first extracted from both treated and untreated mitochondria and then its quantification was carried out by an enzymatic assay previously described [21]: 0.6 ml of 1 M KOH in ethanol were added to the resuspended mitochondria and the mixture was kept at RT for 30 min and then cooled on ice for 10 min. After the addition of 1 ml of a solution containing 0.5 M triethanolamine, 0.4 M KH<sub>2</sub>PO<sub>4</sub>, and 0.1 M K<sub>2</sub>HPO<sub>4</sub>, the suspension

was kept for 10 min at RT and then centrifuged at 33000 x g for 20 min. The amount of NADH was assessed fluorimetrically by the following enzymatic assay:



(reaction catalyzed by the enzyme lactate dehydrogenase).

The reaction begins after the addition of 50 mM Na-Pyruvate and 1  $\mu\text{l}$  lactate dehydrogenase (10 units) in 2 ml of pyridine nucleotide extract.

*Determination of GSH levels* - Mitochondria (4 mg, 2 mg/ml) were treated with DA and Ty as described above. After centrifugation, mitochondria were resuspended in 2 ml incubation buffer, 400  $\mu\text{l}$  of cold 18%  $\text{HClO}_4$  and 400  $\mu\text{l}$  of 2.1 M  $\text{K}_3\text{PO}_4$ . The resulted suspension was allowed to stand on ice 15 min prior to centrifugation at 30000 rpm for 15 min. GSH levels were measured by an enzymatic recycling procedure in which GSH was sequentially oxidized by 6 mM of 5,5-dithio-bis-(2-nitrobenzoic acid) and reduced by 0.3 mM NADPH in the presence of 50 units/ml of glutathione reductase. The rate of 2-nitro-5-thiobenzoic formation was monitored at 412 nm using a spectrophotometer and the concentration of GSH was determined using a standard curve that was generated with known amounts of GSH [18, 21].

*UV-vis spectroscopy* - Spectra were recorded on a personal computer-interfaced diode array Agilent 8453 UV-visible spectrophotometer. Optical measurements were performed under continuous stirring at 25 °C using HELLMA quartz cells with Suprasil windows and an optical path length of 1 cm. The wavelength range was 190-1100 nm. In a first series of experiments, 40  $\mu\text{M}$  DA was dissolved in 20 mM phosphate buffer (pH 7.4) in the absence or presence of different amounts (40, 80 and 160  $\mu\text{M}$ ) of NADH or GSH or both chemicals. Spectra were then recorded for 10 min at 30 s intervals after the addition of 100 units of Ty. In a second series, 100 units of Ty were added to the solution containing 40  $\mu\text{M}$  DA and the reaction was carried out for 5 min before the addition of NADH or GSH or both chemicals. Then, spectra were acquired for 60 min at 2 min intervals.

*NMR spectroscopy* - NMR spectra were recorded on a Bruker Avance DMX600 spectrometer equipped with a gradient triple resonance probe. The NMR experiments, consisting of 16K data points, were carried out at 298 K. The spectral width was set to 7183.91 Hz and the frequency offset to 2820.3 Hz. Prior to Fourier transformation, the time domain data were multiplied by an exponential function and zero filling to 32K points was employed to increase the digital resolution. Sodium 3-(trimethylsilyl)propionate-2,2,3,3- $\text{d}_4$  (TSP) was used as an internal chemical shift reference. Stock solutions of the reagents were obtained by dissolving them in 99.9%  $\text{D}_2\text{O}$ . Samples were then prepared by mixing the stock solutions to obtain the desired final concentrations. Two series of experiments were carried out. In the first one, DA was dissolved in 20 mM phosphate (pH 7.4) to a final concentration of 150  $\mu\text{M}$  in the presence of 600  $\mu\text{M}$  NADH or GSH or

both chemicals. Spectra were recorded before and at several time intervals after the addition of 100 units of Ty. In the second series, DA (to a final concentration of 150  $\mu\text{M}$ ) was first added to the reaction medium in the presence of 100 units of Ty and the reaction was carried out for 5 min before the addition of NADH or GSH or both reagents to a final concentration of 600  $\mu\text{M}$ . Then, the reactions were followed by recording a series of one-dimensional spectra at 2 min intervals. An initial delay of about 3 min was necessary for thermal equilibration of the sample and for probe tuning and field shimming.

ACCEPTED MANUSCRIPT

## Results

*Mitochondrial swelling induced by DAQ* - The ability of DAQ to induce permeability transition has been previously reported [8]. This phenomenon is due to the opening of a proteinaceous pore that forms, under certain conditions, in the inner mitochondrial membrane making mitochondria permeable to solutes of molecular mass up to 1500 Da [22]. In a previous work, Costantini et al. provided evidence that two distinct thiols can modulate PT through their redox state [18]. One of these thiols is sensitive to the redox state of the PN pool in the mitochondrial matrix (labeled P site), when the other is in equilibrium with the redox state of the GSH pool in the matrix (labeled S site).

Here, we first verified the induction of liver mitochondrial swelling after DAQ exposure (Fig. 1A). By the addition of CsA, a specific inhibitor of PT, we also verified that the swelling is really due to the opening of the mitochondrial permeability transition pore (mPTP). Then, to better understand the mechanism through which DAQ induce PT, we repeated the experiments in the presence of two different alkylating agents that block the thiol groups at the P or S site with different selectivity [18]. Specifically, preincubation of the mitochondria with monobromobimane (MBB) or N-ethylmaleimide (NEM) results in the alkylation of the S site thiols or both the S and the P thiols, respectively. When the S thiols are blocked with MBB, DAQ are still able to induce PT. On the contrary, when P thiols are blocked with NEM, DAQ are no more able to induce PT (Fig. 1A). This result suggests that DAQ can induce the opening of the mPTP *via* a mechanism that involves thiols in equilibrium with the PN pool. Comparable results were obtained with mitochondria from mice forebrain (see Fig. 1 supplementary material).

*DAQ-induced effect on GSH and NADH pools* - To assess the redox state of the GSH and the NADH pools in the mitochondria matrix after DAQ exposure, mitochondria were incubated with DA in the presence of Ty for 10 minutes; the incubation buffer (see Materials and Methods) contained CsA to inhibit the mitochondrial permeability transition and the release of GSH or NADH from mitochondria. Subsequently, GSH and NADH levels were determined from DAQ-treated and untreated mitochondria on acid and alkaline extracts, respectively, and the fractions of reduced molecules were quantified and compared to the control. While incubation of mitochondria with DAQ did not affect reduced GSH levels, exposure to DAQ led to the oxidation of NADH in the mitochondrial matrix (Fig. 1B). Parallel experiments performed with only Ty or DA did not show any change in NADH levels. As a further control the GSSG levels were also quantified without showing any significant increase upon DAQ treatment (data not shown). These results

suggest that DAQ can oxidize NADH in the mitochondrial matrix, while they do not affect GSH level.

*DAQ reactivity toward NADH and GSH* - To assess whether DAQ could react with NADH directly, the reactivity was followed by UV-vis and NMR spectroscopy. The competitive reactivity of GSH was also taken into account. In the data presented here, a fourfold molar excess of NADH or GSH relative to DA was used, although experiments using different molar ratios were also performed (data not shown).

The oxidation of DA generates three monomeric quinone species, dopamine-o-quinone (DQ), aminochrome (AC) and indole-5,6-quinone (IQ) [23], which are all potentially reactive in a cellular environment. While the spectroscopic characterization of IQ is still elusive, DA, DQ and AC possess characteristic UV-vis peaks with absorption maxima at 280 (DA), 390 (DQ) and 300/480 (AC) nm [7]. As previously reported [7], during the Ty-mediated oxidation of DA at physiological pH and 25 °C only AC is detectable in the optical spectra with no evidence for the presence of DQ. This can be rationalized on the basis of the high reactivity of DQ that undergoes an intramolecular cyclization reaction with a rate constant of  $\sim 0.15 \text{ s}^{-1}$  [24]. On the contrary, the rearrangement reaction which involves AC to form 5,6-dihydroxyindole (DHI), with a rate constant of  $\sim 0.06 \text{ min}^{-1}$ , is much slower leading to accumulation of AC [23]. Also NADH possesses a characteristic absorption peak centered at 340 nm so that its oxidation can be easily detected by a decrease of the signal at 340 nm.

After verifying that DA does not react directly with NADH (data not shown), Ty was added to the solution. The subsequent formation of DAQ was accompanied by the consumption of NADH (Fig. 2A). The comparison of the kinetic profile of AC appearance, after the addition of Ty in the presence or absence of NADH, indicates that NADH reduced the rate of AC accumulation (Fig. 2B). It is worth mentioning that the appearance of a peak at 480 nm was concomitant, not consequent to the consumption of NADH indicating that, under these experimental conditions, DQ cyclization proceeded at a rate comparable with that of its reduction by NADH. The effects of GSH were then analyzed. The rate constant of the nucleophilic addition of GSH to DQ has been described to be three orders of magnitude greater than the cyclization reaction, with a rate constant of  $\sim 200 \text{ s}^{-1}$  [24]. In agreement, after the addition of Ty to a solution containing both DA and GSH, peaks relative to AC did not appear while two new peaks at 256 and 292 nm became visible (Suppl. Material-1). According to Nicolis et al., they were assigned to glutathionyl-DA adducts [25]. The higher reactivity of GSH toward DQ, relative to NADH, was further confirmed by mixing together DA, GSH and NADH before the addition of Ty. During the evolution of the reaction, NADH was not consumed while a slight increase of the absorbance at  $\sim 292 \text{ nm}$  suggested the formation of

GSH-DA adducts (Suppl. Material-Fig. 2). Our UV data indicated the occurrence of a redox reaction between DQ and NADH, concomitant to the DQ cyclization reaction. In the presence of GSH, however, these reactions did not occur because the nucleophilic attack of GSH on DQ was largely favored.

To confirm the UV-vis results, the reactivity of DQ toward NADH and GSH was also analyzed by NMR spectroscopy. A considerable advantage of the NMR approach proposed here is the possibility to observe the time evolution of the different species independently. Furthermore, aggregation processes do not complicate the analysis of the spectra. In analogy with the UV characterization, the reactivity of DQ, the first quinone formed after oxidation of dopamine, was analyzed in a first series of experiments. For the sake of clarity, only the most informative region of the NMR spectra is presented in Fig. 3. For this reason, peaks corresponding to GSH, which resonate at lower ppm, are not shown in the figure. Peak assignment was carried out by exploiting information available in the literature [23, 25-27]. The spectrum of DA and NADH recorded before the addition of Ty revealed the presence in solution of a small amount of  $\text{NAD}^+$ , as a contaminant of the commercial NADH (Fig. 3A). Nevertheless, the limited concentration of  $\text{NAD}^+$  did not substantially interfere with the analysis. In agreement with the UV data, 4 min after the addition of Ty, peaks corresponding to NADH disappeared while peaks relative to  $\text{NAD}^+$  became much more visible in the spectrum. A decrease in intensity of DA peaks was also visible, indicating that, concomitant with the consumption of NADH, quinone species were also formed. These species were not visible in the spectrum because of their low concentration and of their transient nature. The situation did not evolve further in the spectrum recorded after 10 min, most likely because of the complete consumption of the molecular oxygen dissolved in solution. When GSH was used instead of NADH, the behaviour was very different (Fig. 3B). After the addition of Ty, DA peaks fully disappeared while two new peaks became visible, which were unambiguously assigned to the 5-S-glutathionyl-DA [25]. Furthermore, NADH added after the formation of the GSH-DA adduct was not oxidized to  $\text{NAD}^+$ . The competitive action of NADH and GSH toward DQ was investigated next (Fig. 3C). When Ty was added to a solution containing DA, NADH and GSH, the disappearance of DA peaks was accompanied only by the appearance of peaks corresponding to the 5-S-glutathionyl-DA derivative while NADH and  $\text{NAD}^+$  peak intensities were not affected. In conclusion, in agreement with the UV analysis, NMR data indicated the presence of a redox reaction involving DQ and NADH, but when GSH was present, the reaction between DQ and GSH to form a covalent adduct was strongly favoured.

*AC and IQ reactivity toward NADH and GSH* - To obtain a more detailed description of the DAQ reactivity, the reactions that involve AC and IQ were analyzed, excluding the reactivity of

DQ. To this aim, Ty was added to a solution containing DA, and NADH or GSH were added 5 min later, to allow the complete enzymatic transformation of DA into AC (and other downstream species). The UV-vis spectra recorded in the control experiment, i.e., in the absence of either NADH or GSH, are shown in Fig. 4A. The time evolution of AC could be followed at 300 nm while it was more difficult to extrapolate at 480 nm. In fact, as we have already described in a previous work, light scattering increases during the reaction, as a consequence of the polymerization process [23]. Although light scattering complicated the analysis when NADH was added to the solution, its consumption was still evident, as shown in Fig. 4B. In contrast to the behaviour observed in the case of AC alone or after the addition of NADH, when GSH was added to the solution, light scattering did not appear (Fig. 4C) indicating that the polymerization process was blocked by the formation of a stable adduct. At the same time, the rearrangement rate of AC was not perturbed by the presence of GSH, suggesting that AC is not reactive toward GSH. As a direct consequence, IQ appeared to be the earliest reactive quinone species toward GSH. The competitive reactivity of GSH and NADH was finally analyzed by the simultaneous addition of both chemicals to a solution containing AC (Fig. 4D). As already observed in the case of DQ, the presence of GSH prevented the consumption of NADH. Considering the sequential temporal appearance of AC and IQ, if GSH reactivity involved only IQ, as our data suggested, it follows that also NADH consumption observed in the absence of GSH derived from a redox reaction involving only IQ. In conclusion, the UV-vis data indicated that while AC did not show any reactivity toward either NADH or GSH, IQ was able to react with both NADH and GSH. As in the case of DQ, the nucleophilic attack of GSH on IQ was largely favored.

To confirm these observations through a different experimental strategy, pseudo-2D NMR experiments were recorded (Fig. 5). The top view of the NMR spectra presented here offers the advantage to easily follow the kinetic evolution of the different species present in solution. Even more importantly, by setting the threshold just above the instrumental noise, peaks corresponding to low-concentration species, otherwise difficult to follow, can be emphasized. The drawback is the loss of information about the relative peak intensities so that an additional analysis of the temporal evolution of the peak intensities may be required. As a control, a delay of 5 min after the addition of Ty was first verified to be sufficient to fully convert DA in AC without the concomitant presence of DQ (data not shown). When NADH was added to the solution 5 min after Ty, peaks corresponding to AC still disappeared (Fig. 5A), similar to the behaviour described in a previous work in the absence of NADH [23]. Oxidation of NADH also occurred, as indicated by the kinetic profiles of NADH disappearance and  $\text{NAD}^+$  formation (Suppl. Material- Fig. 3A). The time evolution of the peak intensities also indicated that the oxidation of NADH took place until AC was

present in solution, and then it stopped. As AC decay is the rate limiting step during the polymerization process, these data could not be used to specifically assign the observed reactivity to AC or IQ. In the presence of GSH instead of NADH (Fig. 5B), AC disappearance was followed by the growth of three new peaks that were assigned to 4-S-glutathionyl-DHI, according to Segura-Aguilar et al [28]. As already suggested by our UV analysis, the nature of this adduct indicated that AC did not show any reactivity toward GSH, while IQ did. The results obtained by UV spectroscopy were also confirmed when NADH and GSH were put together in solution after the formation of AC (Fig. 5C). Once again, the AC disappearance was accompanied by the formation of 4S-GSH-DHI. Although the presence of peaks corresponding to  $\text{NAD}^+$  might suggest a redox reaction between quinones and NADH, this effect is a consequence of the top view representation and of the initial presence of  $\text{NAD}^+$  as a contaminant. This becomes evident by analyzing the kinetic profiles of NADH consumption and  $\text{NAD}^+$  formation (Suppl. Material- Fig. 3B). In conclusion, the NMR data fully confirmed our UV-vis results: IQ was able to react with both NADH and GSH, but the nucleophilic attack of GSH on IQ was largely favored. In contrast, AC did not show any reactivity toward either NADH or GSH.

ACCEPTED

## Discussion

Studies of patients with PD demonstrate a 35% decrease in mitochondrial electron transport chain (ETC) complex I activity in the SN region [3, 29]. As DA is able to inhibit respiration in isolated brain mitochondria in a dose-dependent manner [8, 30, 31], this has raised the speculation that DA may bring about mitochondrial dysfunction within DA-neurons by the same mechanisms mediating inhibition in isolated mitochondria [8, 30]. DA reactivity could be linked to chemical modification of ETC sulfhydryls through pathways involving oxidative reactions or covalent adduct formation [8]. The ability of DAQ to induce permeability transition has also been reported [8]. With the aim of shedding some light on the mechanism through which DAQ can induce PT, the first goal of the present work is the analysis of the redox state of the GSH and NADH pool in mitochondria exposed to DAQ. Our results show that DAQ exposure causes the oxidation of NADH in the mitochondrial matrix, while both the reduced GSH and oxidized GSSG levels are not affected. This is in agreement with data obtained by incubating human neuroblastoma SH-SY5Y cells in the presence of DA [32]. These results suggest a possible mechanism of toxicity of DAQ in mitochondria, involving the oxidation of NADH, which can lead to a variety of toxic effects. In addition to promoting the opening of the mPTP, PN oxidation could also affect the activity of the ETC, particularly at the level of complex I. In fact, the electrons derived from NADH oxidation by complex I flow through the ETC to generate the proton gradient, which is then used by the ATP synthase complex to produce ATP from ADP and Pi.

Metabolism of DA in dopaminergic neurons is a complex process, which involves the production of reactive oxygen species, quinone species and polymeric products. For this reason, an unequivocal characterization of the chemical species responsible for mitochondrial dysfunction is far from easy. Nevertheless, data from the literature emphasise the involvement of quinone products in the inactivation of complex I and complex IV [9, 10] and in the opening of the mPTP [8]. In this context, the second goal of this work is the molecular characterization, *in vitro*, of the DA-derived quinone reactivity toward NADH and GSH. The oxidation of DA generates three monomeric quinone species, DQ, AC and IQ [23], which are all potentially reactive in a cellular environment.

The results obtained in the present work are summarized in Fig. 6. Dopamine-derived quinone reactivity has been usually ascribed to DQ. Actually, this electron-deficient species reacts very fast with the cysteinyl residues of proteins while the reactions of the other nucleophilic amino acids are too slow to compete with its intramolecular cyclization [24]. Here, not only the expected reactivity of DQ toward GSH was confirmed, but we also documented the occurrence of a redox reaction between DQ and NADH. IQ is also very reactive as indicated by the fact that, to our

knowledge, it has never been isolated and it does not accumulate in solution at concentrations high enough to be detected by the techniques used here (approximately 20  $\mu\text{M}$ ). In fact, as soon as IQ is formed, it undergoes an auto-condensation reaction to form a black precipitate. In this study, we demonstrated that IQ reacts with GSH as well as with NADH.

Several reports in the literature associate experimental toxic effects, observed on cellular viability or proteasomal dysfunction, to AC [32-35]. This seems to contrast with the data presented here, which indicate that AC does not react either with NADH or with GSH. It should be mentioned that it is hard to discriminate between the reactivity of AC and that of IQ. Indeed, in most published studies the investigators added freshly prepared AC to their reaction mixture without taking into account the possibility of the subsequent spontaneous rearrangement reaction which involves AC to form DHI, which can be further oxidized to IQ. A way to deal with this issue has been to associate the toxic effects observed to products defined as “cyclized DA-derived quinones” [34, 35]. To further support our proposal, in a very recent study the reaction between GSH and AC was analyzed by HPLC and mass spectroscopy [36]. Although the investigators still purported the formation of GSH-AC conjugates, they pointed out a discrepancy with their mass spectrometry data, which could be rationalized by assuming the reaction between GSH and IQ to form glutathionyl-DHI adducts.

In conclusion, the data presented in this work indicate a very diverse behaviour for the different DAQ studied. Specifically, DQ and IQ are very reactive with both NADH and GSH even though the reaction with GSH is largely favoured. On the contrary, AC does not show any apparent reactivity. The higher reactivity of GSH toward quinones, observed *in vitro*, poses an interesting question on why GSH does not prevent NADH oxidation inside mitochondria.

One plausible explanation for the oxidation of NADH is that this is not coming from a direct interaction with DAQ, but through ROS-mediated oxidation. In agreement with this hypothesis, Zoccarato et al. demonstrated that incubation of respiring brain mitochondria with DAQ generates  $\text{O}_2^{\cdot-}/\text{H}_2\text{O}_2$  [37]. The site of  $\text{O}_2^{\cdot-}/\text{H}_2\text{O}_2$  production appeared to be the inner face of the inner mitochondrial membrane. An observation relevant to the reactivity presented here is that peroxide production was not prevented by GSH [37]. Another possible explanation is an indirect effect of DAQ on NADH, mediated by the P-site thiols. In this framework, PN oxidation could be a consequence of a selective interaction of DAQ with the P thiols, whose redox state depends on an equilibrium with the PN pool.

**Acknowledgments**

We would like to thank Prof. Paolo Bernardi for helpful discussions and for critical reading of the manuscript. This work was supported by grants from the University of Padova (PRAT2008), from the “Bruno Kessler” foundation and the MIUR (PRIN2008).

ACCEPTED MANUSCRIPT

## Bibliography

1. Dorsey, E. R., Constantinescu, R., Thompson, J. P., Biglan, K. M., Holloway, R. G., Kieburtz, K., Marshall, F. J., Ravina, B. M., Schifitto, G., Siderowf, A. & Tanner, C. M. (2007) Projected number of people with Parkinson disease in the most populous nations, 2005 through 2030, *Neurology*. *68*, 384-6.
2. Sulzer, D. (2007) Multiple hit hypotheses for dopamine neuron loss in Parkinson's disease, *Trends Neurosci*. *30*, 244-50.
3. Schapira, A. H., Cooper, J. M., Dexter, D., Clark, J. B., Jenner, P. & Marsden, C. D. (1990) Mitochondrial complex I deficiency in Parkinson's disease, *J Neurochem*. *54*, 823-7.
4. Hirsch, E. C. (1993) Does oxidative stress participate in nerve cell death in Parkinson's disease?, *Eur Neurol*. *33 Suppl 1*, 52-9.
5. Jenner, P. (1998) Oxidative mechanisms in nigral cell death in Parkinson's disease, *Mov Disord*. *13 Suppl 1*, 24-34.
6. Jenner, P. & Olanow, C. W. (1998) Understanding cell death in Parkinson's disease, *Ann Neurol*. *44*, S72-84.
7. Graham, D. G. (1978) Oxidative pathways for catecholamines in the genesis of neuromelanin and cytotoxic quinones, *Mol Pharmacol*. *14*, 633-43.
8. Berman, S. B. & Hastings, T. G. (1999) Dopamine oxidation alters mitochondrial respiration and induces permeability transition in brain mitochondria: implications for Parkinson's disease, *J Neurochem*. *73*, 1127-37.
9. Gluck, M. R. & Zeevalk, G. D. (2004) Inhibition of brain mitochondrial respiration by dopamine and its metabolites: implications for Parkinson's disease and catecholamine-associated diseases, *J Neurochem*. *91*, 788-95.
10. Khan, F. H., Sen, T., Maiti, A. K., Jana, S., Chatterjee, U. & Chakrabarti, S. (2005) Inhibition of rat brain mitochondrial electron transport chain activity by dopamine oxidation products during extended in vitro incubation: implications for Parkinson's disease, *Biochim Biophys Acta*. *1741*, 65-74.
11. Jana, S., Maiti, A. K., Bagh, M. B., Banerjee, K., Das, A., Roy, A. & Chakrabarti, S. (2007) Dopamine but not 3,4-dihydroxy phenylacetic acid (DOPAC) inhibits brain respiratory chain activity by autoxidation and mitochondria catalyzed oxidation to quinone products: implications in Parkinson's disease, *Brain Res*. *1139*, 195-200.
12. Dringen, R., Gutterer, J. M. & Hirrlinger, J. (2000) Glutathione metabolism in brain metabolic interaction between astrocytes and neurons in the defense against reactive oxygen species, *Eur J Biochem*. *267*, 4912-6.
13. Sohal, R. S. & Weindruch, R. (1996) Oxidative stress, caloric restriction, and aging, *Science*. *273*, 59-63.
14. Kang, Y., Viswanath, V., Jha, N., Qiao, X., Mo, J. Q. & Andersen, J. K. (1999) Brain gamma-glutamyl cysteine synthetase (GCS) mRNA expression patterns correlate with regional-specific enzyme activities and glutathione levels, *J Neurosci Res*. *58*, 436-41.
15. Riederer, P., Sofic, E., Rausch, W. D., Schmidt, B., Reynolds, G. P., Jellinger, K. & Youdim, M. B. (1989) Transition metals, ferritin, glutathione, and ascorbic acid in parkinsonian brains, *J Neurochem*. *52*, 515-20.
16. Jenner, P., Dexter, D. T., Sian, J., Schapira, A. H. & Marsden, C. D. (1992) Oxidative stress as a cause of nigral cell death in Parkinson's disease and incidental Lewy body disease. The Royal Kings and Queens Parkinson's Disease Research Group, *Ann Neurol*. *32 Suppl*, S82-7.
17. Spencer, J. P., Jenner, P. & Halliwell, B. (1995) Superoxide-dependent depletion of reduced glutathione by L-DOPA and dopamine. Relevance to Parkinson's disease, *Neuroreport*. *6*, 1480-4.
18. Costantini, P., Chernyak, B. V., Petronilli, V. & Bernardi, P. (1996) Modulation of the mitochondrial permeability transition pore by pyridine nucleotides and dithiol oxidation at two separate sites, *J Biol Chem*. *271*, 6746-51.
19. Chernyak, B. V. & Bernardi, P. (1996) The mitochondrial permeability transition pore is modulated by oxidative agents through both pyridine nucleotides and glutathione at two separate sites, *Eur J Biochem*. *238*, 623-30.
20. Costantini, P., Petronilli, V., Colonna, R. & Bernardi, P. (1995) On the effects of paraquat on isolated mitochondria. Evidence that paraquat causes opening of the cyclosporin A-sensitive permeability transition pore synergistically with nitric oxide, *Toxicology*. *99*, 77-88.
21. Beatrice, M. C., Stiers, D. L. & Pfeiffer, D. R. (1984) The role of glutathione in the retention of Ca<sup>2+</sup> by liver mitochondria, *J Biol Chem*. *259*, 1279-87.
22. Bernardi, P., Broekemeier, K. M. & Pfeiffer, D. R. (1994) Recent progress on regulation of the mitochondrial permeability transition pore; a cyclosporin-sensitive pore in the inner mitochondrial membrane, *J Bioenerg Biomembr*. *26*, 509-17.
23. Bisaglia, M., Mammi, S. & Bubacco, L. (2007) Kinetic and structural analysis of the early oxidation products of dopamine: analysis of the interactions with alpha-synuclein, *J Biol Chem*. *282*, 15597-605.
24. Tse, D. C., McCreery, R. L. & Adams, R. N. (1976) Potential oxidative pathways of brain catecholamines, *J Med Chem*. *19*, 37-40.
25. Nicolis, S., Zucchelli, M., Monzani, E. & Casella, L. (2008) Myoglobin modification by enzyme-generated dopamine reactive species, *Chemistry*. *14*, 8661-73.
26. Yang, X., Bi, S., Yang, L., Zhu, Y. & Wang, X. (2003) Multi-NMR and fluorescence spectra study the effects of aluminum(III) on coenzyme NADH in aqueous solutions, *Spectrochim Acta A Mol Biomol Spectrosc*. *59*, 2561-9.
27. Yang, X., Bi, S., Yang, L., Hu, J., Liu, J. & Yang, Z. (2003) NMR spectra and potentiometry studies of aluminum(III) binding with coenzyme NAD<sup>+</sup> in acidic aqueous solutions, *Anal Sci*. *19*, 815-21.

28. Segura-Aguilar, J., Baez, S., Widersten, M., Welch, C. J. & Mannervik, B. (1997) Human class Mu glutathione transferases, in particular isoenzyme M2-2, catalyze detoxication of the dopamine metabolite aminochrome, *J Biol Chem.* 272, 5727-31.
29. Parker, W. D., Jr., Boyson, S. J. & Parks, J. K. (1989) Abnormalities of the electron transport chain in idiopathic Parkinson's disease, *Ann Neurol.* 26, 719-23.
30. Cohen, G., Farooqui, R. & Kesler, N. (1997) Parkinson disease: a new link between monoamine oxidase and mitochondrial electron flow, *Proc Natl Acad Sci U S A.* 94, 4890-4.
31. Gluck, M., Ehrhart, J., Jayatilleke, E. & Zeevalk, G. D. (2002) Inhibition of brain mitochondrial respiration by dopamine: involvement of H<sub>2</sub>O<sub>2</sub> and hydroxyl radicals but not glutathione-protein-mixed disulfides, *J Neurochem.* 82, 66-74.
32. Gimenez-Xavier, P., Gomez-Santos, C., Castano, E., Francisco, R., Boada, J., Unzeta, M., Sanz, E. & Ambrosio, S. (2006) The decrease of NAD(P)H has a prominent role in dopamine toxicity, *Biochim Biophys Acta.* 1762, 564-74.
33. Diaz-Veliz, G., Mora, S., Dossi, M. T., Gomez, P., Arriagada, C., Montiel, J., Aboitiz, F. & Segura-Aguilar, J. (2002) Behavioral effects of aminochrome and dopachrome injected in the rat substantia nigra, *Pharmacol Biochem Behav.* 73, 843-50.
34. Zafar, K. S., Siegel, D. & Ross, D. (2006) A potential role for cyclized quinones derived from dopamine, DOPA, and 3,4-dihydroxyphenylacetic acid in proteasomal inhibition, *Mol Pharmacol.* 70, 1079-86.
35. Zhou, Z. D. & Lim, T. M. (2009) Dopamine (DA) induced irreversible proteasome inhibition via DA derived quinones, *Free Radic Res.* 43, 417-30.
36. Zhou, Z. D. & Lim, T. M. (2009) Roles of glutathione (GSH) in dopamine (DA) oxidation studied by improved tandem HPLC plus ESI-MS, *Neurochem Res.* 34, 316-26.
37. Zoccarato, F., Toscano, P. & Alexandre, A. (2005) Dopamine-derived dopaminochrome promotes H<sub>2</sub>O<sub>2</sub> release at mitochondrial complex I: stimulation by rotenone, control by Ca<sup>2+</sup>, and relevance to Parkinson disease, *J Biol Chem.* 280, 15587-94.

ACCEPTED

**Figure legends**

Figure 1. DAQ effects on mitochondrial swelling and on reduced glutathione and NADH pools. A) Mitochondria swelling was measured after treatment with DAQ. The effect of CsA, NEM and MBB were also taken into account. B) The amounts of reduced GSH and NADH in isolated mitochondria were assessed after treatment with DAQ and compared to the untreated control. Values are the mean  $\pm$  SEM (n = 3)

Figure 2. UV-vis spectral changes associated with the reactions between NADH and DAQ. A) To make the graphical visualization easier, selected spectra are shown, recorded at 1 minute intervals after the addition of Ty to a solution containing NADH and DA. B) Time dependence of the variation in absorbance of NADH (filled circles) and AC (filled triangles) after the addition of Ty. Open triangles represent the temporal evolution of AC in the absence of NADH.

Figure 3. NMR analysis of DQ reactivity. 1D-NMR spectra were recorded after the addition of Ty to a solution containing DA and A) NADH, B) GSH, and C) both NADH and GSH. DA peaks are represented in black, NADH peaks in blue, NAD<sup>+</sup> peaks in red and 5-S-glutathionyl-DA in green.

Figure 4. Competitive reactions of NADH and GSH with AC and IQ. To make the graphical visualization easier, selected UV-vis spectra are shown, recorded at 10 minute intervals after the addition of NADH and/or GSH to a solution containing AC. A) Spectral evolution of AC peaks in the absence of both NADH and GSH. Light scattering appears during the course of the reaction. B) NADH consumption is visible after its addition to the solution containing AC, in spite of the presence of light scattering. The inset represents the time evolution of the peak corresponding to NADH. C) Addition of GSH blocks light scattering formation, but does not alter AC decay. D) The concomitant presence of GSH prevents the consumption of NADH.

Upward arrows, downward arrows and left-right double arrowheads indicate, respectively, a temporal increase, decrease and invariance of the spectral feature assigned to the indicated chemical species. In panel A, a significant increase in light scattering is observed.

Figure 5. NMR analysis of AC and IQ reactivity. Pseudo 2D-NMR spectra were recorded at 2 minute intervals. To permit the complete enzymatic transformation of DA into AC, Ty and DA were mixed together 5 minutes before the subsequent addition of A) NADH, B) GSH, or C) both NADH and GSH. AC peaks are represented in black, NADH peaks in blue, NAD<sup>+</sup> peaks in red and 4-S-glutathionyl-DHI in green.

Figure 6. Schematic representation of the reactions studied. DQ and IQ react with both NADH and GSH, but the reaction with GSH is largely favoured. In contrast, AC does not show any reactivity. In agreement with this picture, while DQ and IQ do not accumulate in solution because of their reactivity, AC rearrangement is much slower and permits its accumulation.

ACCEPTED MA

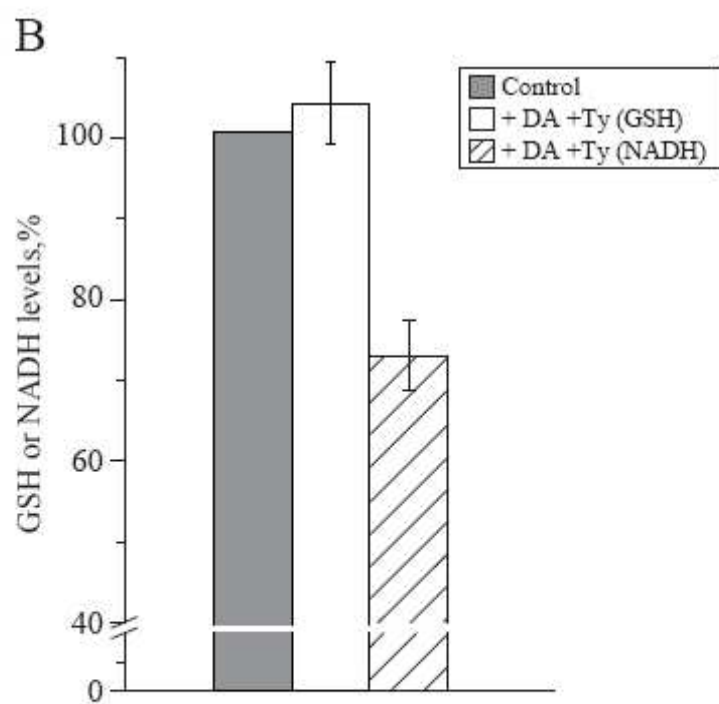
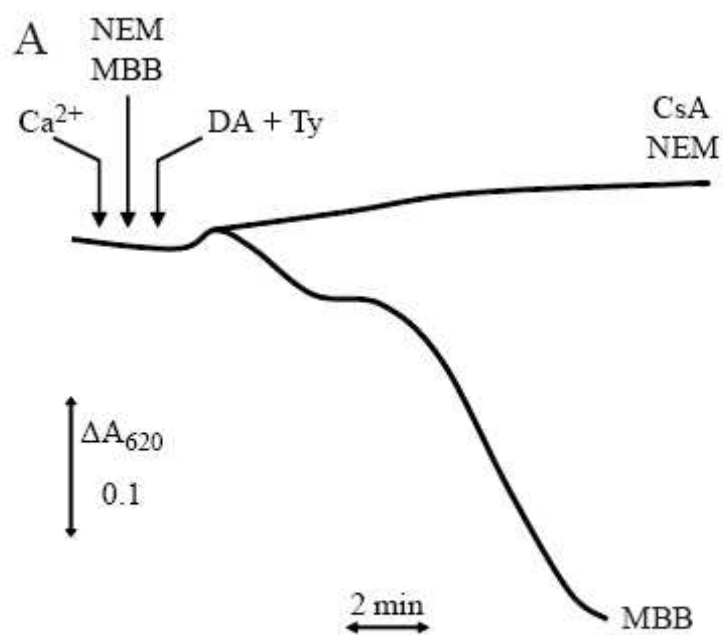


Fig. 1

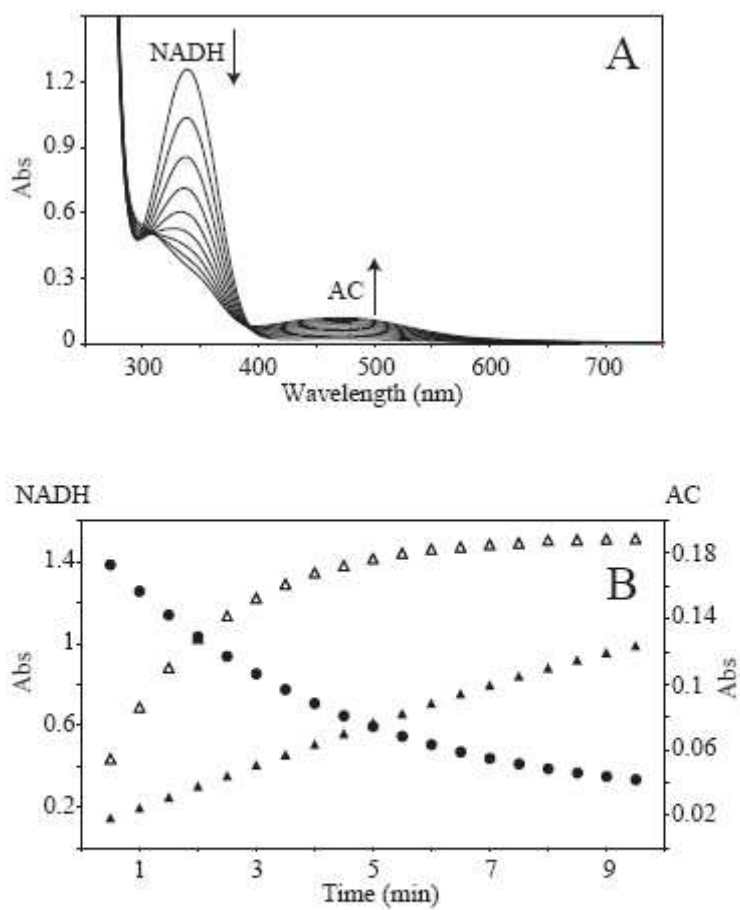


Fig. 2

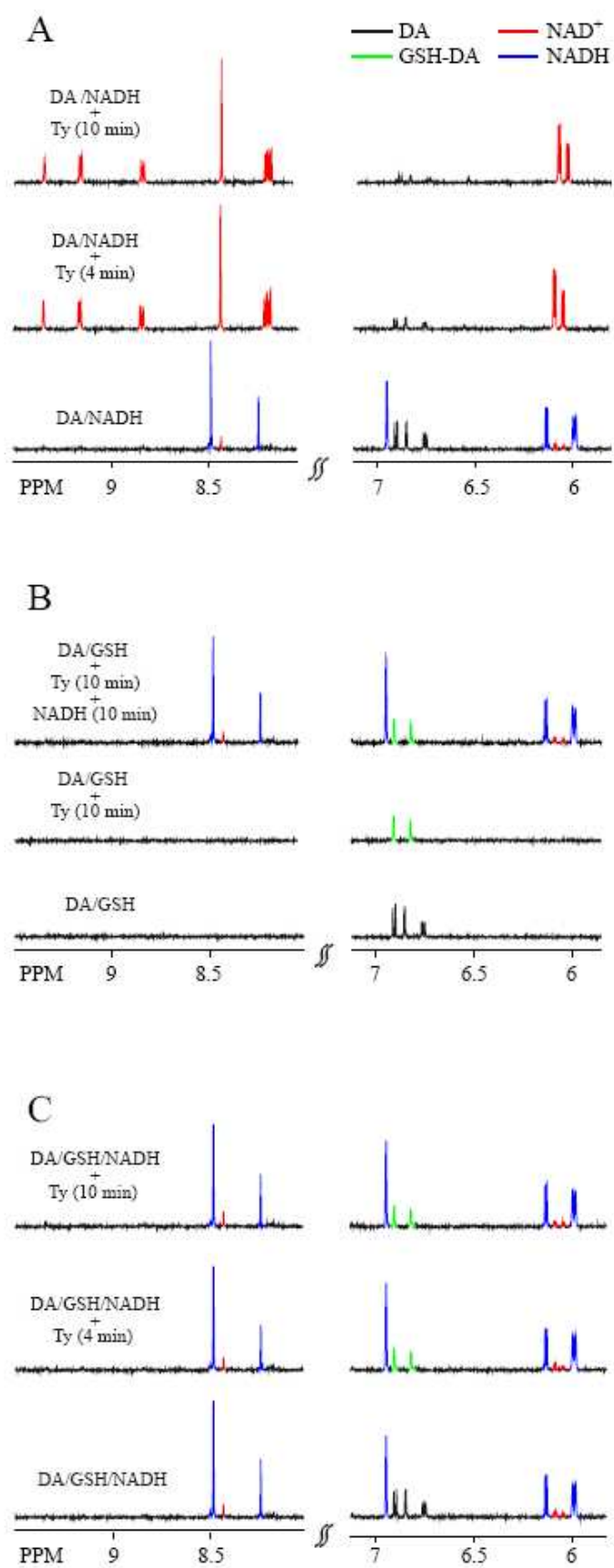


Fig. 3

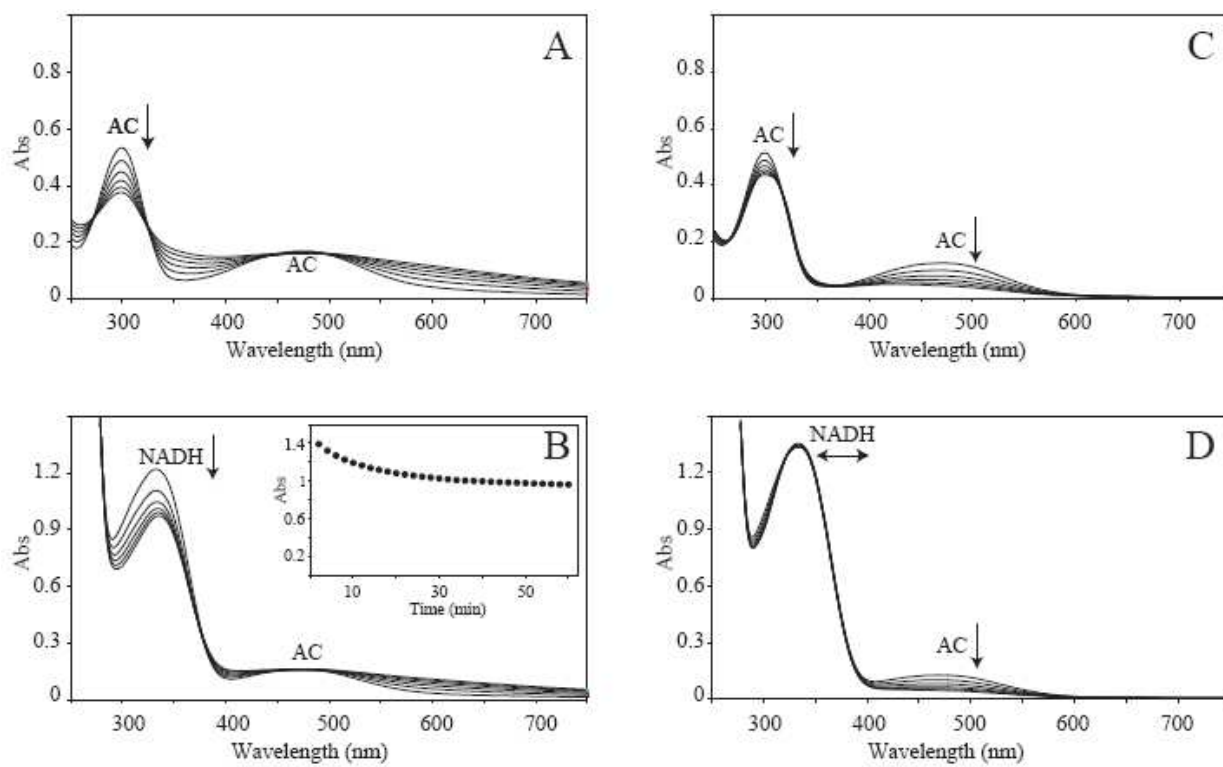


Fig. 4

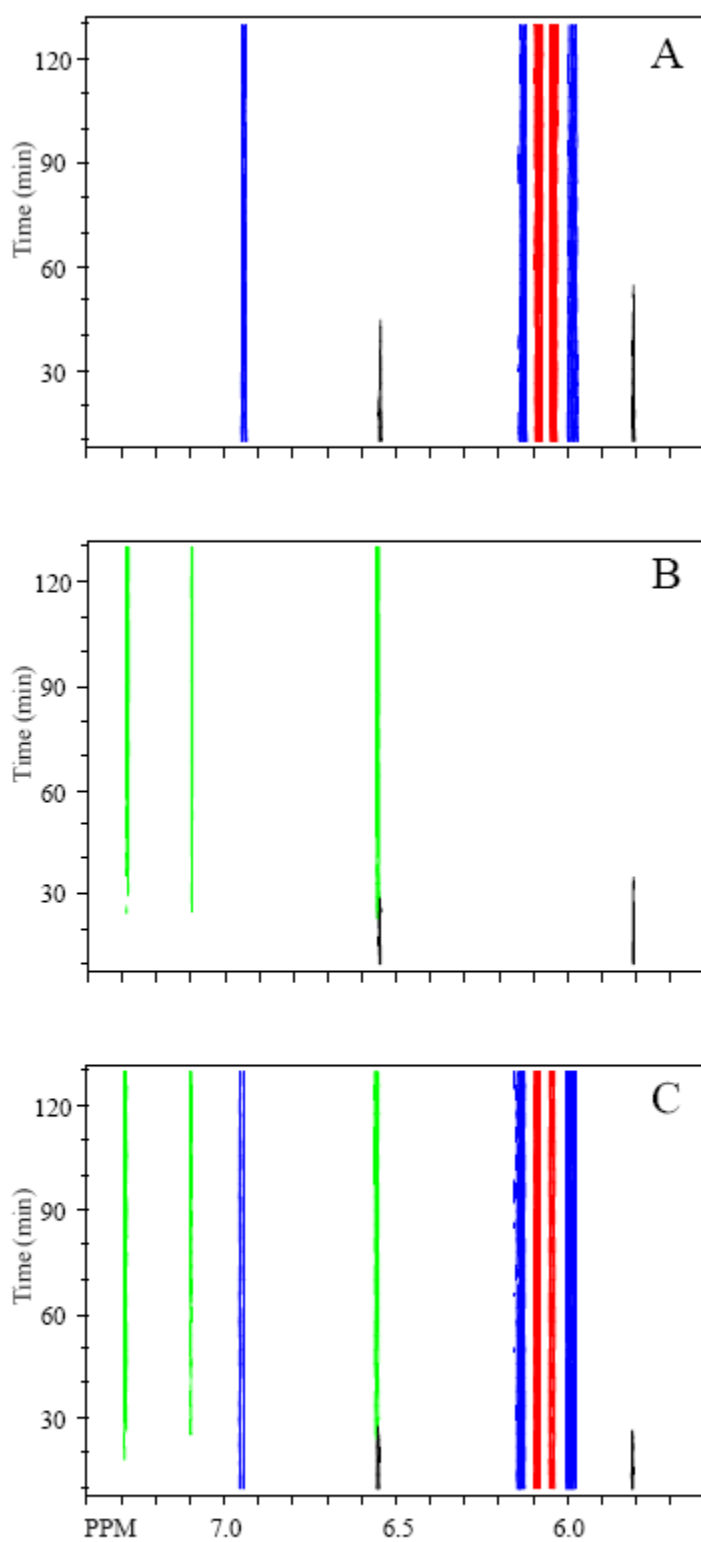


Fig. 5

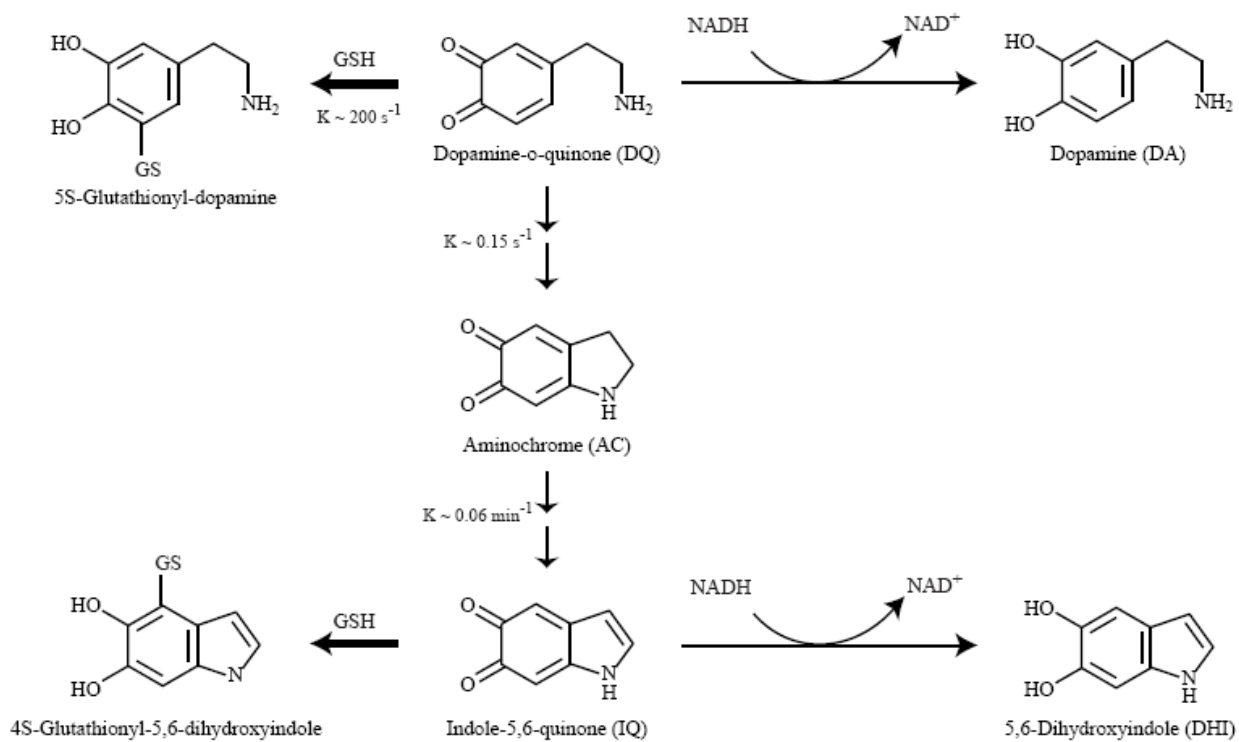


Fig. 6